BABAR-PUB-03/015
SLAC-PUB-9986

Measurement of Time-Dependent CP Asymmetries and the CP-Odd Fraction in the Decay $B^0 \to D^{*+}D^{*-}$

B. Aubert,[1] R. Barate,[1] D. Boutigny,[1] J.-M. Gaillard,[1] A. Hicheur,[1] Y. Karyotakis,[1] J. P. Lees,[1] P. Robbe,[1] V. Tisserand,[1] A. Zghiche,[1] A. Palano,[2] A. Pompili,[2] J. C. Chen,[3] N. D. Qi,[3] G. Rong,[3] P. Wang,[3] Y. S. Zhu,[3] G. Eigen,[4] I. Ofte,[4] B. Stugu,[4] G. S. Abrams,[5] A. W. Borgland,[5] A. B. Breon,[5] D. N. Brown,[5] J. Button-Shafer,[5] R. N. Cahn,[5] E. Charles,[5] C. T. Day,[5] M. S. Gill,[5] A. V. Gritsan,[5] Y. Groysman,[5] R. G. Jacobsen,[5] R. W. Kadel,[5] J. Kadyk,[5] L. T. Kerth,[5] Yu. G. Kolomensky,[5] J. F. Kral,[5] G. Kukartsev,[5] C. LeClerc,[5] M. E. Levi,[5] G. Lynch,[5] L. M. Mir,[5] P. J. Oddone,[5] T. J. Orimoto,[5] M. Pripstein,[5] N. A. Roe,[5] A. Romosan,[5] M. T. Ronan,[5] V. G. Shelkov,[5] A. V. Telnov,[5] W. A. Wenzel,[5] K. Ford,[6] T. J. Harrison,[6] C. M. Hawkes,[6] D. J. Knowles,[6] S. E. Morgan,[6] R. C. Penny,[6] A. T. Watson,[6] N. K. Watson,[6] T. Deppermann,[7] K. Goetzen,[7] H. Koch,[7] B. Lewandowski,[7] M. Pelizaeus,[7] K. Peters,[7] H. Schmuecker,[7] M. Steinke,[7] N. R. Barlow,[8] J. T. Boyd,[8] N. Chevalier,[8] W. N. Cottingham,[8] M. P. Kelly,[8] T. E. Latham,[8] C. Mackay,[8] F. F. Wilson,[8] K. Abe,[9] T. Cuhadar-Donszelmann,[9] C. Hearty,[9] T. S. Mattison,[9] J. A. McKenna,[9] D. Thiessen,[9] P. Kyberd,[10] A. K. McKemey,[10] V. E. Blinov,[11] A. D. Bukin,[11] V. B. Golubev,[11] V. N. Ivanchenko,[11] E. A. Kravchenko,[11] A. P. Onuchin,[11] S. I. Serednyakov,[11] Yu. I. Skovpen,[11] E. P. Solodov,[11] A. N. Yushkov,[11] D. Best,[12] M. Chao,[12] D. Kirkby,[12] A. J. Lankford,[12] M. Mandelkern,[12] S. McMahon,[12] R. K. Mommsen,[12] W. Roethel,[12] D. P. Stoker,[12] C. Buchanan,[13] D. del Re,[14] H. K. Hadavand,[14] E. J. Hill,[14] D. B. MacFarlane,[14] H. P. Paar,[14] Sh. Rahatlou,[14] U. Schwanke,[14] V. Sharma,[14] J. W. Berryhill,[15] C. Campagnari,[15] B. Dahmes,[15] N. Kuznetsova,[15] S. L. Levy,[15] O. Long,[15] A. Lu,[15] M. A. Mazur,[15] J. D. Richman,[15] W. Verkerke,[15] T. W. Beck,[16] J. Beringer,[16] A. M. Eisner,[16] C. A. Heusch,[16] W. S. Lockman,[16] T. Schalk,[16] R. E. Schmitz,[16] B. A. Schumm,[16] A. Seiden,[16] M. Turri,[16] W. Walkowiak,[16] D. C. Williams,[16] M. G. Wilson,[16] J. Albert,[17] E. Chen,[17] G. P. Dubois-Felsmann,[17] A. Dvoretskii,[17] D. G. Hitlin,[17] I. Narsky,[17] F. C. Porter,[17] A. Ryd,[17] A. Samuel,[17] S. Yang,[17] S. Jayatilleke,[18] G. Mancinelli,[18] B. T. Meadows,[18] M. D. Sokoloff,[18] T. Abe,[19] T. Barillari,[19] F. Blanc,[19] P. Bloom,[19] S. Chen,[19] P. J. Clark,[19] W. T. Ford,[19] U. Nauenberg,[19] A. Olivas,[19] P. Rankin,[19] J. Roy,[19] J. G. Smith,[19] W. C. van Hoek,[19] L. Zhang,[19] J. L. Harton,[20] T. Hu,[20] A. Soffer,[20] W. H. Toki,[20] R. J. Wilson,[20] J. Zhang,[20] D. Altenburg,[21] T. Brandt,[21] J. Brose,[21] T. Colberg,[21] M. Dickopp,[21] R. S. Dubitzky,[21] A. Hauke,[21] H. M. Lacker,[21] E. Maly,[21] R. Müller-Pfefferkorn,[21] R. Nogowski,[21] S. Otto,[21] K. R. Schubert,[21] R. Schwierz,[21] B. Spaan,[21] L. Wilden,[21] D. Bernard,[22] G. R. Bonneaud,[22] F. Brochard,[22] J. Cohen-Tanugi,[22] Ch. Thiebaux,[22] G. Vasileiadis,[22] M. Verderi,[22] A. Khan,[23] D. Lavin,[23] F. Muheim,[23] S. Playfer,[23] J. E. Swain,[23] J. Tinslay,[23] M. Andreotti,[24] V. Azzolini,[24] D. Bettoni,[24] C. Bozzi,[24] R. Calabrese,[24] G. Cibinetto,[24] E. Luppi,[24] M. Negrini,[24] L. Piemontese,[24] A. Sarti,[24] E. Treadwell,[25] F. Anulli,[26,*] R. Baldini-Ferroli,[26] A. Calcaterra,[26] R. de Sangro,[26] D. Falciai,[26] G. Finocchiaro,[26] P. Patteri,[26] I. M. Peruzzi,[26,*] M. Piccolo,[26] A. Zallo,[26] A. Buzzo,[27] R. Contri,[27] G. Crosetti,[27] M. Lo Vetere,[27] M. Macri,[27] M. R. Monge,[27] S. Passaggio,[27] F. C. Pastore,[27] C. Patrignani,[27] E. Robutti,[27] A. Santroni,[27] S. Tosi,[27] S. Bailey,[28] M. Morii,[28] W. Bhimji,[29] D. A. Bowerman,[29] P. D. Dauncey,[29] U. Egede,[29] I. Eschrich,[29] J. R. Gaillard,[29] G. W. Morton,[29] J. A. Nash,[29] P. Sanders,[29] G. P. Taylor,[29] G. J. Grenier,[30] S.-J. Lee,[30] U. Mallik,[30] J. Cochran,[31] H. B. Crawley,[31] J. Lamsa,[31] W. T. Meyer,[31] S. Prell,[31] E. I. Rosenberg,[31] J. Yi,[31] M. Davier,[32] G. Grosdidier,[32] A. Höcker,[32] S. Laplace,[32] F. Le Diberder,[32] V. Lepeltier,[32] A. M. Lutz,[32] T. C. Petersen,[32] S. Plaszczynski,[32] M. H. Schune,[32] L. Tantot,[32] G. Wormser,[32] V. Brigljević,[33] C. H. Cheng,[33] D. J. Lange,[33] D. M. Wright,[33] A. J. Bevan,[34] J. P. Coleman,[34] J. R. Fry,[34] E. Gabathuler,[34] R. Gamet,[34] M. Kay,[34] R. J. Parry,[34] D. J. Payne,[34] R. J. Sloane,[34] C. Touramanis,[34] J. J. Back,[35] P. F. Harrison,[35] H. W. Shorthouse,[35] P. Strother,[35] P. B. Vidal,[35] C. L. Brown,[36] G. Cowan,[36] R. L. Flack,[36] H. U. Flaecher,[36] S. George,[36] M. G. Green,[36] A. Kurup,[36] C. E. Marker,[36] T. R. McMahon,[36] S. Ricciardi,[36] F. Salvatore,[36] G. Vaitsas,[36] M. A. Winter,[36] D. Brown,[37] C. L. Davis,[37] J. Allison,[38] R. J. Barlow,[38] P. A. Hart,[38] A. C. Forti,[38] F. Jackson,[38] G. D. Lafferty,[38] A. J. Lyon,[38] J. H. Weatherall,[38] J. C. Williams,[38] A. Farbin,[39] A. Jawahery,[39] D. Kovalskyi,[39] C. K. Lae,[39] V. Lillard,[39] D. A. Roberts,[39] G. Blaylock,[40] C. Dallapiccola,[40] K. T. Flood,[40] S. S. Hertzbach,[40] R. Kofler,[40] V. B. Koptchev,[40] T. B. Moore,[40] S. Saremi,[40] H. Staengle,[40] S. Willocq,[40] R. Cowan,[41] G. Sciolla,[41] F. Taylor,[41] R. K. Yamamoto,[41] D. J. J. Mangeol,[42] M. Milek,[42] P. M. Patel,[42]

A. Lazzaro,[43] F. Palombo,[43] J. M. Bauer,[44] L. Cremaldi,[44] V. Eschenburg,[44] R. Godang,[44] R. Kroeger,[44] J. Reidy,[44] D. A. Sanders,[44] D. J. Summers,[44] H. W. Zhao,[44] C. Hast,[45] P. Taras,[45] H. Nicholson,[46] C. Cartaro,[47] N. Cavallo,[47,†] G. De Nardo,[47] F. Fabozzi,[47,†] C. Gatto,[47] L. Lista,[47] P. Paolucci,[47] D. Piccolo,[47] C. Sciacca,[47] M. A. Baak,[48] G. Raven,[48] J. M. LoSecco,[49] T. A. Gabriel,[50] B. Brau,[51] T. Pulliam,[51] Q. K. Wong,[51] J. Brau,[52] R. Frey,[52] C. T. Potter,[52] N. B. Sinev,[52] D. Strom,[52] E. Torrence,[52] F. Colecchia,[53] A. Dorigo,[53] F. Galeazzi,[53] M. Margoni,[53] M. Morandin,[53] M. Posocco,[53] M. Rotondo,[53] F. Simonetto,[53] R. Stroili,[53] G. Tiozzo,[53] C. Voci,[53] M. Benayoun,[54] H. Briand,[54] J. Chauveau,[54] P. David,[54] Ch. de la Vaissière,[54] L. Del Buono,[54] O. Hamon,[54] M. J. J. John,[54] Ph. Leruste,[54] J. Ocariz,[54] M. Pivk,[54] L. Roos,[54] J. Stark,[54] S. T'Jampens,[54] G. Therin,[54] P. F. Manfredi,[55] V. Re,[55] L. Gladney,[56] Q. H. Guo,[56] J. Panetta,[56] C. Angelini,[57] G. Batignani,[57] S. Bettarini,[57] M. Bondioli,[57] F. Bucci,[57] G. Calderini,[57] M. Carpinelli,[57] F. Forti,[57] M. A. Giorgi,[57] A. Lusiani,[57] G. Marchiori,[57] F. Martinez-Vidal,[57,‡] M. Morganti,[57] N. Neri,[57] E. Paoloni,[57] M. Rama,[57] G. Rizzo,[57] F. Sandrelli,[57] J. Walsh,[57] M. Haire,[58] D. Judd,[58] K. Paick,[58] D. E. Wagoner,[58] N. Danielson,[59] P. Elmer,[59] C. Lu,[59] V. Miftakov,[59] J. Olsen,[59] A. J. S. Smith,[59] H. A. Tanaka,[59] E. W. Varnes,[59] F. Bellini,[60] G. Cavoto,[59,60] R. Faccini,[14,60] F. Ferrarotto,[60] F. Ferroni,[60] M. Gaspero,[60] M. A. Mazzoni,[60] S. Morganti,[60] M. Pierini,[60] G. Piredda,[60] F. Safai Tehrani,[60] C. Voena,[60] S. Christ,[61] G. Wagner,[61] R. Waldi,[61] T. Adye,[62] N. De Groot,[62] B. Franek,[62] N. I. Geddes,[62] G. P. Gopal,[62] E. O. Olaiya,[62] S. M. Xella,[62] R. Aleksan,[63] S. Emery,[63] A. Gaidot,[63] S. F. Ganzhur,[63] P.-F. Giraud,[63] G. Hamel de Monchenault,[63] W. Kozanecki,[63] M. Langer,[63] G. W. London,[63] B. Mayer,[63] G. Schott,[63] G. Vasseur,[63] Ch. Yeche,[63] M. Zito,[63] M. V. Purohit,[64] A. W. Weidemann,[64] F. X. Yumiceva,[64] D. Aston,[65] R. Bartoldus,[65] N. Berger,[65] A. M. Boyarski,[65] O. L. Buchmueller,[65] M. R. Convery,[65] D. P. Coupal,[65] D. Dong,[65] J. Dorfan,[65] D. Dujmic,[65] W. Dunwoodie,[65] R. C. Field,[65] T. Glanzman,[65] S. J. Gowdy,[65] E. Grauges-Pous,[65] T. Hadig,[65] V. Halyo,[65] T. Hryn'ova,[65] W. R. Innes,[65] C. P. Jessop,[65] M. H. Kelsey,[65] P. Kim,[65] M. L. Kocian,[65] U. Langenegger,[65] D. W. G. S. Leith,[65] S. Luitz,[65] V. Luth,[65] H. L. Lynch,[65] H. Marsiske,[65] S. Menke,[65] R. Messner,[65] D. R. Muller,[65] C. P. O'Grady,[65] V. E. Ozcan,[65] A. Perazzo,[65] M. Perl,[65] S. Petrak,[65] B. N. Ratcliff,[65] S. H. Robertson,[65] A. Roodman,[65] A. A. Salnikov,[65] R. H. Schindler,[65] J. Schwiening,[65] G. Simi,[65] A. Snyder,[65] A. Soha,[65] J. Stelzer,[65] D. Su,[65] M. K. Sullivan,[65] J. Va'vra,[65] S. R. Wagner,[65] M. Weaver,[65] A. J. R. Weinstein,[65] W. J. Wisniewski,[65] D. H. Wright,[65] C. C. Young,[65] P. R. Burchat,[66] A. J. Edwards,[66] T. I. Meyer,[66] C. Roat,[66] S. Ahmed,[67] M. S. Alam,[67] J. A. Ernst,[67] M. Saleem,[67] F. R. Wappler,[67] W. Bugg,[68] M. Krishnamurthy,[68] S. M. Spanier,[68] R. Eckmann,[69] H. Kim,[69] J. L. Ritchie,[69] R. F. Schwitters,[69] J. M. Izen,[70] I. Kitayama,[70] X. C. Lou,[70] S. Ye,[70] F. Bianchi,[71] M. Bona,[71] F. Gallo,[71] D. Gamba,[71] C. Borean,[72] L. Bosisio,[72] G. Della Ricca,[72] S. Dittongo,[72] S. Grancagnolo,[72] L. Lanceri,[72] P. Poropat,[72,§] L. Vitale,[72] G. Vuagnin,[72] R. S. Panvini,[73] Sw. Banerjee,[74] C. M. Brown,[74] D. Fortin,[74] P. D. Jackson,[74] R. Kowalewski,[74] J. M. Roney,[74] H. R. Band,[75] S. Dasu,[75] M. Datta,[75] A. M. Eichenbaum,[75] H. Hu,[75] J. R. Johnson,[75] P. E. Kutter,[75] H. Li,[75] R. Liu,[75] F. Di Lodovico,[75] A. Mihalyi,[75] A. K. Mohapatra,[75] Y. Pan,[75] R. Prepost,[75] S. J. Sekula,[75] J. H. von Wimmersperg-Toeller,[75] J. Wu,[75] S. L. Wu,[75] Z. Yu,[75] and H. Neal[76]

(The *BABAR* Collaboration)

[1]*Laboratoire de Physique des Particules, F-74941 Annecy-le-Vieux, France*
[2]*Università di Bari, Dipartimento di Fisica and INFN, I-70126 Bari, Italy*
[3]*Institute of High Energy Physics, Beijing 100039, China*
[4]*University of Bergen, Inst. of Physics, N-5007 Bergen, Norway*
[5]*Lawrence Berkeley National Laboratory and University of California, Berkeley, CA 94720, USA*
[6]*University of Birmingham, Birmingham, B15 2TT, United Kingdom*
[7]*Ruhr Universität Bochum, Institut für Experimentalphysik 1, D-44780 Bochum, Germany*
[8]*University of Bristol, Bristol BS8 1TL, United Kingdom*
[9]*University of British Columbia, Vancouver, BC, Canada V6T 1Z1*
[10]*Brunel University, Uxbridge, Middlesex UB8 3PH, United Kingdom*
[11]*Budker Institute of Nuclear Physics, Novosibirsk 630090, Russia*
[12]*University of California at Irvine, Irvine, CA 92697, USA*
[13]*University of California at Los Angeles, Los Angeles, CA 90024, USA*
[14]*University of California at San Diego, La Jolla, CA 92093, USA*
[15]*University of California at Santa Barbara, Santa Barbara, CA 93106, USA*
[16]*University of California at Santa Cruz, Institute for Particle Physics, Santa Cruz, CA 95064, USA*
[17]*California Institute of Technology, Pasadena, CA 91125, USA*
[18]*University of Cincinnati, Cincinnati, OH 45221, USA*
[19]*University of Colorado, Boulder, CO 80309, USA*
[20]*Colorado State University, Fort Collins, CO 80523, USA*

[21] Technische Universität Dresden, Institut für Kern- und Teilchenphysik, D-01062 Dresden, Germany
[22] Ecole Polytechnique, LLR, F-91128 Palaiseau, France
[23] University of Edinburgh, Edinburgh EH9 3JZ, United Kingdom
[24] Università di Ferrara, Dipartimento di Fisica and INFN, I-44100 Ferrara, Italy
[25] Florida A&M University, Tallahassee, FL 32307, USA
[26] Laboratori Nazionali di Frascati dell'INFN, I-00044 Frascati, Italy
[27] Università di Genova, Dipartimento di Fisica and INFN, I-16146 Genova, Italy
[28] Harvard University, Cambridge, MA 02138, USA
[29] Imperial College London, London, SW7 2BW, United Kingdom
[30] University of Iowa, Iowa City, IA 52242, USA
[31] Iowa State University, Ames, IA 50011-3160, USA
[32] Laboratoire de l'Accélérateur Linéaire, F-91898 Orsay, France
[33] Lawrence Livermore National Laboratory, Livermore, CA 94550, USA
[34] University of Liverpool, Liverpool L69 3BX, United Kingdom
[35] Queen Mary, University of London, E1 4NS, United Kingdom
[36] University of London, Royal Holloway and Bedford New College, Egham, Surrey TW20 0EX, United Kingdom
[37] University of Louisville, Louisville, KY 40292, USA
[38] University of Manchester, Manchester M13 9PL, United Kingdom
[39] University of Maryland, College Park, MD 20742, USA
[40] University of Massachusetts, Amherst, MA 01003, USA
[41] Massachusetts Institute of Technology, Laboratory for Nuclear Science, Cambridge, MA 02139, USA
[42] McGill University, Montréal, QC, Canada H3A 2T8
[43] Università di Milano, Dipartimento di Fisica and INFN, I-20133 Milano, Italy
[44] University of Mississippi, University, MS 38677, USA
[45] Université de Montréal, Laboratoire René J. A. Lévesque, Montréal, QC, Canada H3C 3J7
[46] Mount Holyoke College, South Hadley, MA 01075, USA
[47] Università di Napoli Federico II, Dipartimento di Scienze Fisiche and INFN, I-80126, Napoli, Italy
[48] NIKHEF, National Institute for Nuclear Physics and High Energy Physics, NL-1009 DB Amsterdam, The Netherlands
[49] University of Notre Dame, Notre Dame, IN 46556, USA
[50] Oak Ridge National Laboratory, Oak Ridge, TN 37831, USA
[51] Ohio State University, Columbus, OH 43210, USA
[52] University of Oregon, Eugene, OR 97403, USA
[53] Università di Padova, Dipartimento di Fisica and INFN, I-35131 Padova, Italy
[54] Universités Paris VI et VII, Lab de Physique Nucléaire H. E., F-75252 Paris, France
[55] Università di Pavia, Dipartimento di Elettronica and INFN, I-27100 Pavia, Italy
[56] University of Pennsylvania, Philadelphia, PA 19104, USA
[57] Università di Pisa, Dipartimento di Fisica, Scuola Normale Superiore and INFN, I-56127 Pisa, Italy
[58] Prairie View A&M University, Prairie View, TX 77446, USA
[59] Princeton University, Princeton, NJ 08544, USA
[60] Università di Roma La Sapienza, Dipartimento di Fisica and INFN, I-00185 Roma, Italy
[61] Universität Rostock, D-18051 Rostock, Germany
[62] Rutherford Appleton Laboratory, Chilton, Didcot, Oxon, OX11 0QX, United Kingdom
[63] DSM/Dapnia, CEA/Saclay, F-91191 Gif-sur-Yvette, France
[64] University of South Carolina, Columbia, SC 29208, USA
[65] Stanford Linear Accelerator Center, Stanford, CA 94309, USA
[66] Stanford University, Stanford, CA 94305-4060, USA
[67] State Univ. of New York, Albany, NY 12222, USA
[68] University of Tennessee, Knoxville, TN 37996, USA
[69] University of Texas at Austin, Austin, TX 78712, USA
[70] University of Texas at Dallas, Richardson, TX 75083, USA
[71] Università di Torino, Dipartimento di Fisica Sperimentale and INFN, I-10125 Torino, Italy
[72] Università di Trieste, Dipartimento di Fisica and INFN, I-34127 Trieste, Italy
[73] Vanderbilt University, Nashville, TN 37235, USA
[74] University of Victoria, Victoria, BC, Canada V8W 3P6
[75] University of Wisconsin, Madison, WI 53706, USA
[76] Yale University, New Haven, CT 06511, USA

(Dated: July 13, 2011)

We present a measurement of time-dependent CP asymmetries and an updated determination of the CP-odd fraction in the decay $B^0 \to D^{*+}D^{*-}$ using a data sample of $88 \times 10^6 B\bar{B}$ pairs collected by the BABAR detector at the PEP-II B Factory at SLAC. We determine the CP-odd fraction to be $0.063 \pm 0.055(\mathrm{stat}) \pm 0.009(\mathrm{syst})$. The time-dependent CP asymmetry parameters $\mathrm{Im}(\lambda_+)$ and $|\lambda_+|$ are determined to be $0.05 \pm 0.29(\mathrm{stat}) \pm 0.10(\mathrm{syst})$ and $0.75 \pm 0.19(\mathrm{stat}) \pm 0.02(\mathrm{syst})$, respectively.

The Standard Model predicts these parameters to be $-\sin 2\beta$ and 1, respectively, in the absence of penguin diagram contributions.

PACS numbers: 13.25.Hw, 12.15.Hh, 11.30.Er

The symmetry for combined charge conjugation *(C)* and parity *(P)* transformations is violated in B decays. Measurements of *CP* asymmetries by the *BABAR* [1] and BELLE [2] collaborations established this effect and are compatible with the Standard Model expectation based on the current knowledge of the Cabibbo-Kobayashi-Maskawa [3] quark-mixing matrix. As a result of the interference between direct B decay and decay after flavor change, a *CP*-violating asymmetry is expected in the time evolution of the decays $B^0 \to D^{*+}D^{*-}$ [4] within the framework of the Standard Model [5]. This *CP* asymmetry is related to $\sin 2\beta$ when corrections due to theoretically uncertain penguin diagram contributions are neglected [6, 7]. Penguin-induced corrections are predicted to be small in models based on the factorization approximation and heavy-quark symmetry; an effect of about 2% is predicted by Ref. [8]. A comparison of measurements of $\sin 2\beta$ from $b \to c\bar{c}s$ modes such as $B^0 \to J/\psi K^0_S$ [9] with that obtained in $B^0 \to D^{*+}D^{*-}$ is an important test of these models and the Standard Model.

The $B^0 \to D^{*+}D^{*-}$ mode is a pseudoscalar decay to a vector-vector final state, with contributions from three partial waves with different *CP* parities: even for the S- and D-waves, odd for the P-wave. The *CP*-odd contribution is predicted to be about 5.5% in Ref. [10]. We present an updated [11] determination of the *CP*-odd fraction, $R_\perp$, based on a one-dimensional time-integrated angular analysis. We also present a measurement of the time-dependent *CP* asymmetry, obtained from a combined analysis of the time dependence of flavor-tagged decays and the one-dimensional angular distribution of the decay products. The data used in this analysis were collected with the *BABAR* detector at the PEP-II storage ring. The *BABAR* detector is described in detail elsewhere [12]. The data sample corresponds to about 88×10^6 $e^+e^- \to \Upsilon(4S) \to B\bar{B}$ events.

B^0 mesons are exclusively reconstructed by combining two charged D^* candidates reconstructed in the modes $D^{*+} \to D^0\pi^+$ and $D^{*+} \to D^+\pi^0$. We include the $D^{*+}D^{*-}$ combinations $(D^0\pi^+, \overline{D}^0\pi^-)$ and $(D^0\pi^+, D^-\pi^0)$, but not $(D^+\pi^0, D^-\pi^0)$ due to the smaller branching fraction and larger backgrounds. Prior to forming a B^0, the D^* candidates are subjected to a mass-constrained fit and vertex fit that includes the position of the beam spot.

The reconstructed D^0 and D^+ modes are $D^0 \to K^-\pi^+$, $K^-\pi^+\pi^0$, $K^-\pi^+\pi^+\pi^-$, $K^0_S\pi^+\pi^-$, and $D^+ \to K^-\pi^+\pi^+$, $K^0_S\pi^+$, $K^-K^+\pi^+$. The reconstructed mass of the D^0 (D^+) candidates is required to be within 20 MeV/c^2 of the nominal D^0 (D^+) mass [13], except for $D^0 \to K^-\pi^+\pi^0$, which has a looser requirement of 35 MeV/c^2. The D candidates are subjected to a mass-constrained fit prior to forming D^* candidates.

Charged kaon candidates are required to be inconsistent with the pion hypothesis, as inferred from the Cherenkov angle measured by the Cherenkov detector and the specific ionization measured by the charged-particle tracking system. No particle identification requirements are made for the kaon from the decay $D^0 \to K^-\pi^+$. The reconstructed mass of $K^0_S \to \pi^+\pi^-$ candidates is required to be within 25 MeV/c^2 of the nominal K^0_S mass. The angle between the flight direction and the momentum vector of the K^0_S is required to be less than 200 mrad, and the transverse flight distance from the primary event vertex must be greater than 2 mm. A mass-constrained fit is applied to each K^0_S candidate. Neutral pion candidates are formed from two photons detected in the electromagnetic calorimeter, each with energy above 30 MeV; the mass of the pair must be within 20 MeV/c^2 of the nominal π^0 mass, and their summed energy must be greater than 200 MeV. A mass-constrained fit is applied to these π^0 candidates. The mass of the π^0 from $D^{*+} \to D^+\pi^0$, however, is required to be within 35 MeV/c^2 of the nominal π^0 mass, and the momentum in the $\Upsilon(4S)$ frame in the interval $70 < |p^*| < 450$ MeV/c, with no requirement on the photon energy sum.

We construct a mass likelihood $\mathcal{L}_{\rm Mass}$ that includes the mass and mass uncertainty of the D and D^* candidates. The D mass resolution is modeled by a Gaussian whose variance is determined on a candidate-by-candidate basis. The $D^* - D$ mass difference resolution is modeled by a double-Gaussian distribution whose parameters are determined from simulated events. The value of $\mathcal{L}_{\rm Mass}$ is used to select B^0 candidates, with a different requirement used for each D decay mode combination. In an event where more than one B^0 candidate is reconstructed, the candidate with the largest $\mathcal{L}_{\rm Mass}$ value is chosen.

The primary variables used to distinguish signal from background are the energy-substituted mass, $m_{\rm ES} \equiv \sqrt{E^2_{\rm Beam} - p^2_B}$, and the difference of the B candidate energy from the beam energy, $\Delta E \equiv E_B - E_{\rm Beam}$, where all variables are evaluated in the $\Upsilon(4S)$ center-of-mass frame. The B^0 candidates are required to have $-39 < \Delta E < 31$ MeV and $m_{\rm ES} > 5.2$ GeV/c^2.

To reject backgrounds from the $e^+e^- \to c\overline{c}$ continuum process, events are required to have a ratio of second to zeroth Fox-Wolfram moments [14] of less than 0.6. We also require that the cosine of the angle between the thrust axis of the reconstructed B and the thrust axis of the rest of the event be less than 0.9.

After all selection criteria have been applied, a fit to the $m_{\rm ES}$ distribution using a Gaussian and an ARGUS function [15] for the signal and background, respectively, results in a signal yield of $156 \pm 14(\mathrm{stat})$ events. In the region $m_{\mathrm{ES}} > 5.27\ \mathrm{GeV}/c^2$, the signal purity is 73%.

We perform a one-dimensional angular analysis to determine the fraction, $R_\perp$, of the P-wave, CP-odd component of the $B^0 \to D^{*+}D^{*-}$ decay. In the transversity basis [5], the following three angles are defined: the angle θ_1 between the momentum of the slow pion from the D^{*-} in the D^{*-} rest frame and the direction of flight of the D^{*-} in the B rest frame; the polar angle θ_{tr} between the normal to the D^{*-} decay plane and the direction of flight of the slow pion from the D^{*+} in the D^{*+} rest frame; and the corresponding azimuthal angle ϕ_{tr}. The time-dependent angular distribution of the decay products is given in Ref. [16].

The dependence of the detector efficiency on the decay angles can introduce a bias in the measured value of $R_\perp$. Including the efficiency explicitly in the decay rate and then integrating over time and the angles θ_1 and ϕ_{tr} results in the one-dimensional differential decay rate:

$$\begin{aligned}\frac{1}{\Gamma}\frac{d\Gamma}{d\cos\theta_{\mathrm{tr}}} &= \frac{9}{32\pi}\Big[(1-R_\perp)\sin^2\theta_{\mathrm{tr}} \\ &\times \left\{\frac{1+\alpha}{2}I_0(\cos\theta_{\mathrm{tr}}) + \frac{1-\alpha}{2}I_\parallel(\cos\theta_{\mathrm{tr}})\right\} \\ &+ 2R_\perp\cos^2\theta_{\mathrm{tr}} \times I_\perp(\cos\theta_{\mathrm{tr}})\Big], \qquad (1)\end{aligned}$$

where $R_\perp = M_\perp^2/(M_0^2 + M_\parallel^2 + M_\perp^2)$, $\alpha = (M_0^2 - M_\parallel^2)/(M_0^2 + M_\parallel^2)$, and $(M_0, M_\parallel, M_\perp)$ are the magnitudes of the amplitudes in the transversity basis. The three efficiency moments, I_k $(k = 0, \parallel, \perp)$, are defined as

$$I_k(\cos\theta_{\mathrm{tr}}) = \int d\cos\theta_1\, d\phi_{\mathrm{tr}}\ g_k(\theta_1,\phi_{\mathrm{tr}})\,\epsilon(\theta_1,\theta_{\mathrm{tr}},\phi_{\mathrm{tr}}), \quad (2)$$

where $g_0 = 4\cos^2\theta_1\cos^2\phi_{\mathrm{tr}}$, $g_{||} = 2\sin^2\theta_1\sin^2\phi_{\mathrm{tr}}$, $g_\perp = \sin^2\theta_1$, and ϵ is the detector efficiency. The efficiency moments are determined using simulated events. The efficiency moments are fit to second-order even polynomials in $\cos\theta_{\mathrm{tr}}$, the parameters of which are fixed in the subsequent likelihood fit to the $\cos\theta_{\mathrm{tr}}$ distribution.

The measurement of $R_\perp$ is based on a combined unbinned maximum likelihood fit of the $\cos\theta_{\mathrm{tr}}$ and m_{ES} distributions. The probability density function (pdf) for the m_{ES} distribution is given by the sum of ARGUS and Gaussian functions. The background shape is modeled by an even second-order polynomial in $\cos\theta_{\mathrm{tr}}$. The pdf used for signal events is given by Eq. 1. The experimental resolution of θ_{tr} is not negligible and is accounted for by convolving the signal pdf with a double Gaussian. Also, the resolution of θ_{tr} has significant tails caused by mis-reconstructed events. The effect of these tails is accounted for by an additional term in the signal pdf. The parameterization of the θ_{tr} resolution is determined from simulations.

We categorize our events in three types: $D^{*+}D^{*-} \to (D^0\pi^+, \overline{D}^0\pi^-)$, $(D^0\pi^+, D^-\pi^0)$, and $(D^+\pi^0, \overline{D}^0\pi^-)$ because events with a neutral slow pion and events with a charged slow pion have different background levels, detection efficiencies, and $\cos\theta_{\mathrm{tr}}$ resolutions. Thus, the parameters determined in the likelihood fit are three signal fractions, the $\cos\theta_{\mathrm{tr}}$ background shape parameter, three m_{ES} parameters (σ and mean of the Gaussian, and κ from the ARGUS function), and $R_\perp$. The fit to the dataset yields a value of

$$R_\perp = 0.063 \pm 0.055(\mathrm{stat}) \pm 0.009(\mathrm{syst}). \qquad (3)$$

Figure 1 shows the distribution of $\cos\theta_{\mathrm{tr}}$ for events in the range $m_{\mathrm{ES}} > 5.27\ \mathrm{GeV}/c^2$. The value of α is fixed to zero in the fit, incurring a (negligible) systematic uncertainty. The largest systematic uncertainties arise from the parameterization of the angular resolution (0.005) and the determination of the efficiency moments (0.005).

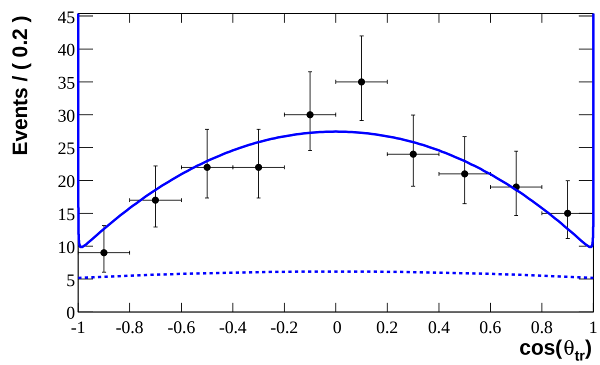

FIG. 1: Measured distribution of $\cos\theta_{\mathrm{tr}}$ and fit results. The data points are from the region $m_{\mathrm{ES}} > 5.27\ \mathrm{GeV}/c^2$ and the solid line is the projection of the fit result in the same region. The dotted line represents the background component.

In addition to the time-independent measurement of the CP-odd fraction, we perform a combined analysis of the $\cos\theta_{\mathrm{tr}}$ distribution and the time dependence in order to determine the time-dependent CP asymmetry, using the sample of $B^0 \to D^{*+}D^{*-}$ events described previously. We also use information from the other B meson in the event to tag its flavor as either a B^0 or $\overline{B}^0$.

Although factorization models predict a small penguin contamination in the weak phase difference in $\mathrm{Im}(\lambda_f) = -\sin 2\beta$ [8], a sizable penguin contribution cannot *a priori* be excluded. Thus, the value of $\lambda_f = \eta_{CP}\frac{q}{p}\frac{\bar{A}(f)}{A(f)}$ [16] can be different for the three transversity amplitudes ($f = \perp, 0, \parallel$) because of possible different penguin-to-tree ratios. This possibility is explicitly included in the parameterization of the decay rates described here.

The decay rate $F_+(F_-)$ for a neutral B meson tagged as a $B^0(\overline{B}^0)$ is given by

$$\begin{aligned}F_\pm(\Delta t) &= \frac{\mathrm{e}^{-|\Delta t|/\tau_{B^0}}}{4\tau_{B^0}}\Big\{G(1-\tfrac{1}{2}\Delta\mathcal{D}) \mp \\ &\mathcal{D}\left[S\sin(\Delta m_d\Delta t) + C\cos(\Delta m_d\Delta t)\right]\Big\}, (4)\end{aligned}$$

where $\Delta t = t_{\rm rec} - t_{\rm tag}$ is the difference between the proper decay time of the reconstructed B meson ($B_{\rm rec}$) and of the tagging B meson ($B_{\rm tag}$), τ_{B^0} is the B^0 lifetime, and Δm_d is the mass difference determined from the B^0-$\overline{B}^0$ oscillation frequency. The dilution factor, $\mathcal{D} = 1 - 2\omega$, where ω is the average mistag fraction, describes the effect of incorrect tags, and $\Delta\mathcal{D}$ accounts for possible differences in the mistag probabilities for B^0 and $\overline{B}^0$. The G, C and S coefficients are defined as

$$\begin{aligned} G &= \tfrac{3}{4}[(1-R_\perp)\sin^2\theta_{\rm tr} + 2R_\perp\cos^2\theta_{\rm tr}], \qquad (5)\\ C &= \tfrac{3}{4}[(1-R_\perp)\tfrac{1-|\lambda_+|^2}{1+|\lambda_+|^2}\sin^2\theta_{\rm tr} + 2R_\perp\tfrac{1-|\lambda_\perp|^2}{1+|\lambda_\perp|^2}\cos^2\theta_{\rm tr}],\\ S &= -\tfrac{3}{4}[(1-R_\perp)\tfrac{2{\rm Im}(\lambda_+)}{1+|\lambda_+|^2}\sin^2\theta_{\rm tr} - 2R_\perp\tfrac{2{\rm Im}(\lambda_\perp)}{1+|\lambda_\perp|^2}\cos^2\theta_{\rm tr}]. \end{aligned}$$

Because the two *CP*-even transversity amplitudes produce the same distribution in $\cos\theta_{\rm tr}$, we are only sensitive to λ_+, the appropriate average of $\lambda_\parallel$ and λ_0:

$$\begin{aligned} \frac{{\rm Im}(\lambda_+)}{1+|\lambda_+|^2} &= \frac{\frac{{\rm Im}(\lambda_\parallel)}{1+|\lambda_\parallel|^2}M_\parallel^2 + \frac{{\rm Im}(\lambda_0)}{1+|\lambda_0|^2}M_0^2}{M_\parallel^2 + M_0^2},\\ \frac{1-|\lambda_+|^2}{1+|\lambda_+|^2} &= \frac{\frac{1-|\lambda_\parallel|^2}{1+|\lambda_\parallel|^2}M_\parallel^2 + \frac{1-|\lambda_0|^2}{1+|\lambda_0|^2}M_0^2}{M_\parallel^2 + M_0^2}. \qquad (6) \end{aligned}$$

If angular acceptance effects are not taken into account and the *CP*-odd fraction is allowed to float in the fit, then no bias is seen in the resulting value of λ_+ based on simulations. Hence, a dedicated method to correct for detector efficiency is not required. The value of $R_\perp$ obtained is therefore an effective value, which is not identical to the acceptance-corrected value from the time-integrated measurement.

The time interval Δt is calculated from the measured separation Δz between the decay vertex of the reconstructed B meson and the vertex of the flavor-tagging B meson along the collision axis. Events with a Δt uncertainty < 2.5 ps, and a measured $|\Delta t| < 20$ ps are accepted. The mistag fractions and Δt resolution functions are determined from a sample of neutral B decays to flavor eigenstates, $B_{\rm flav}$, as in the sin2β measurement using charmonium decays [9]. Vertex reconstruction, the determination of Δt, and the algorithms used for the determination of the flavor of $B_{\rm tag}$ are described in Refs. [9, 17].

We determine the parameters ${\rm Im}(\lambda_+)$ and $|\lambda_+|$ with a simultaneous unbinned maximum likelihood fit to the Δt distributions of the $B_{\rm rec}$ and $B_{\rm flav}$ tagged samples (Fig. 2). The Δt distribution of the $B_{\rm flav}$ sample evolves according to the known frequency for flavor oscillations in neutral B mesons. The observed magnitude of the *CP* asymmetry in the $B_{\rm rec}$ sample and the flavor oscillation in the $B_{\rm flav}$ sample are reduced by the same factor $\mathcal{D}$ due to flavor mistags. The Δt distributions for the $B_{\rm rec}$ and $B_{\rm flav}$ samples are both convolved with a common Δt resolution function. The $\theta_{\rm tr}$ angular resolution is accounted for in the same way as described previously. Events are assigned signal and background probabilities based on their $m_{\rm ES}$ values. Backgrounds are incorporated with an empirical description of their Δt distributions, containing prompt (zero lifetime) and non-prompt components convolved with a separate resolution function [9].

A total of 38 parameters are varied in the fit: the values of ${\rm Im}(\lambda_+)$ and $|\lambda_+|$ (2), the effective *CP*-odd fraction (1), the average mistag fraction w and the difference Δw between B^0 and $\overline{B}^0$ mistags for each tagging category (8), parameters for the signal Δt resolution (9), and parameters for the background time dependence (7), Δt resolution (3), and mistag fractions (8). Because the *CP*-odd fraction is small, we have little sensitivity to the parameters $|\lambda_\perp|$ and ${\rm Im}(\lambda_\perp)$. Therefore they are fixed to 1.0 and -0.741 [9] respectively. These are the values expected if direct *CP* violation and contributions from penguin diagrams are neglected. The changes in the fitted values of ${\rm Im}(\lambda_+)$ and $|\lambda_+|$ for different input values of ${\rm Im}(\lambda_\perp)$ (varied between -1.0 and 1.0) and $|\lambda_\perp|$ (varied between 0.7 and 1.3) are taken into account as systematic uncertainties. The results obtained from the fit (Fig. 2) are

$$\begin{aligned} {\rm Im}(\lambda_+) &= 0.05 \pm 0.29({\rm stat}) \pm 0.10({\rm syst}) \qquad (7)\\ |\lambda_+| &= 0.75 \pm 0.19({\rm stat}) \pm 0.02({\rm syst}). \qquad (8) \end{aligned}$$

The dominant sources of systematic uncertainty come from the variation of the value of $\lambda_\perp$ (0.056 and 0.008, respectively, for ${\rm Im}(\lambda_+)$ and $|\lambda_+|$), and the level, composition, and *CP* asymmetry of the background (0.078 and 0.005).

If the $B \to D^{*+}D^{*-}$ transition proceeds only through the $b \to c\bar{c}d$ tree amplitude, we expect that ${\rm Im}(\lambda_+) = -\sin 2\beta$ and $|\lambda_+| = 1$. To test this hypothesis, we fix ${\rm Im}(\lambda_+) = -0.741$ [9] and $|\lambda_+| = 1$ and repeat the fit. The observed change in the likelihood corresponds to 2.5 standard deviations (statistical uncertainty only).

In summary, we have reported a measurement of the *CP*-odd fraction and measurements of time-dependent *CP* asymmetries for the decay $B^0 \to D^{*+}D^{*-}$. The measurement of $R_\perp$ supersedes the previous *BABAR* result [11], with a factor of three reduction in the statistical uncertainty, and indicates that $B^0 \to D^{*+}D^{*-}$ is mostly *CP*-even. The time-dependent asymmetries are found to differ slightly from Standard Model predictions with penguin amplitudes ignored.

We are grateful for the excellent luminosity and machine conditions provided by our PEP-II colleagues, and for the substantial dedicated effort from the computing organizations that support *BABAR*. The collaborating institutions wish to thank SLAC for its support and kind hospitality. This work is supported by DOE and NSF (USA), NSERC (Canada), IHEP (China), CEA and CNRS-IN2P3 (France), BMBF and DFG (Germany), INFN (Italy), FOM (The Netherlands), NFR (Norway), MIST (Russia), and PPARC (United Kingdom). Indi-

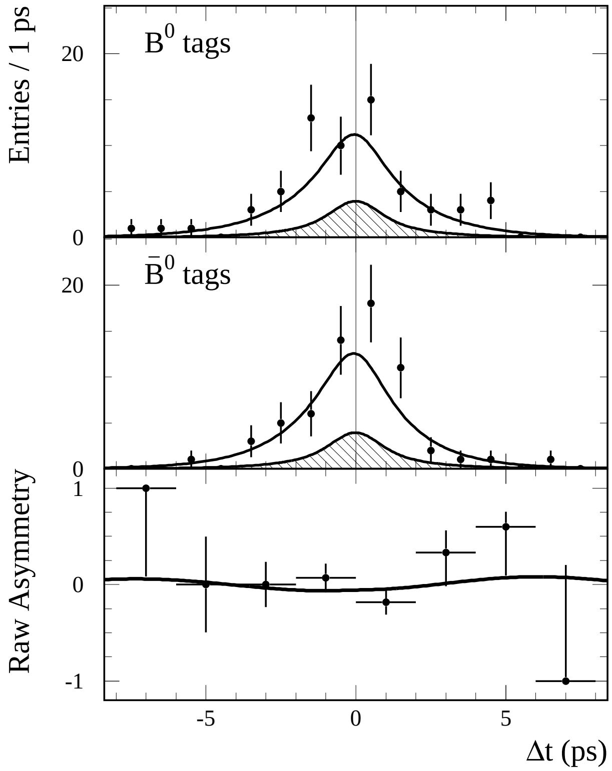

FIG. 2: From top to bottom: Number N_{B^0} ($N_{\overline{B}^0}$) of candidate events in the region $m_{\rm ES} > 5.27$ GeV/c^2 with a B^0 ($\overline{B}^0$) tag, and the raw asymmetry $(N_{B^0} - N_{\overline{B}^0})/(N_{B^0} + N_{\overline{B}^0})$, as functions of Δt. The solid curves represent the result of the combined fit to the full sample. The shaded regions represent the background contributions.

viduals have received support from the A. P. Sloan Foundation, Research Corporation, and Alexander von Humboldt Foundation.

* Also with Università di Perugia, Perugia, Italy

† Also with Università della Basilicata, Potenza, Italy

‡ Also with IFIC, Instituto de Física Corpuscular, CSIC-Universidad de Valencia, Valencia, Spain

§ Deceased

[1] *BABAR* Collaboration, B. Aubert *et al.*, Phys. Rev. Lett. **87**, 091801 (2001).

[2] BELLE Collaboration, K. Abe *et al.*, Phys. Rev. Lett. **87**, 091802 (2001).

[3] N. Cabibbo, Phys. Rev. Lett. **10**, 531 (1963); M. Kobayashi and T. Maskawa, Prog. Th. Phys. **49**, 652 (1973).

[4] Throughout this paper, flavor-eigenstate decay modes also imply their charge conjugate.

[5] I. Dunietz *et al.*, Phys. Rev. D **43**, 2193 (1991).

[6] M. Gronau, Phys. Rev. Lett. **63**, 1451 (1989).

[7] A.I. Sanda and Z.Z. Xing, Phys. Rev. D **56**, 341 (1997).

[8] X.Y. Pham and Z.Z. Xing, Phys. Lett. B **458**, 375 (1999).

[9] *BABAR* Collaboration, B. Aubert *et al.*, Phys. Rev. Lett. **89**, 201802 (2002).

[10] Z.Z. Xing, Phys. Rev. D **61**, 014010 (2000).

[11] *BABAR* Collaboration, B. Aubert *et al.*, Phys. Rev. Lett. **89**, 061801 (2002).

[12] *BABAR* Collaboration, A. Palano *et al.*, Nucl. Instr. and Methods **A479**, 1 (2002).

[13] Particle Data Group, K. Hagiwara *et al.*, Phys. Rev. D **66**, 010001 (2002).

[14] G.C. Fox and S. Wolfram, Phys. Rev. Lett. **41**, 1581 (1978).

[15] Defined as $A \sim \sqrt{x} \times \exp(\kappa x)$ where $x = 1 - (m_{\rm ES}/m_0)^2$ and $m_{\rm ES} < m_0$. The value of m_0 is fixed to 5.291 GeV/c^2. H. Albrecht *et al.*, Z. Phys. C **48**, 543 (1990).

[16] P.F. Harrison and H.R. Quinn, eds. "The *BABAR* Physics Book", SLAC-R504 (1998), Chapter 5, and references therein. (Eq. 5.44 in this reference has wrong signs in the last two terms.)

[17] *BABAR* Collaboration, B.Aubert *et al.*, Phys. Rev. D **66**, 032003 (2002).